plates are evidence of multiple distinct surges of lava or one continuous flow with some temporal variation in flux or flow path. Nonetheless, the features here are very well preserved, indicating that Cerberus Palus is either very young or was buried shortly after formation and recently exhumed.

References and Notes

1. J. B. Murray *et al.*; HRSC Co-Investigator Team, *Nature* **434**, 352 (2005).
2. D. M. Burr, R. J. Soare, J.-M. Wan Bun Tseung, J. P. Emery, *Icarus* **178**, 56 (2005).
3. D. P. Page, *Icarus* **189**, 83 (2007).
4. M. R. Balme, C. Gallagher, *Earth Planet. Sci. Lett.* **285**, 1 (2009).
5. J. B. Plescia, *Icarus* **88**, 465 (1990).
6. L. Keszthelyi, S. Self, T. Thordarson, *J. Geol. Soc. London* **163**, 253 (2006).
7. W. L. Jaeger, L. P. Keszthelyi, A. S. McEwen, C. M. Dundas, P. S. Russell, *Science* **317**, 1709 (2007).
8. L. P. Keszthelyi *et al.*, *Icarus* **205**, 211 (2010).
9. W. L. Jaeger *et al.*, *Icarus* **205**, 230 (2010).
10. W. K. Hartmann, D. C. Berman, *J. Geophys. Res.* **105**, (E6), 15011 (2000).
11. D. M. Burr, J. A. Grier, A. S. McEwen, L. P. Keszthelyi, *Icarus* **159**, 53 (2002).
12. A. McEwen *et al.*, *Icarus* **176**, 351 (2005).
13. J. L. Bandfield, V. E. Hamilton, P. R. Christensen, *Science* **287**, 1626 (2000).
14. P. R. Christensen *et al.*, *J. Geophys. Res.* **106** (E10), 23823 (2001).
15. D. L. Peck, T. Minakami, *Geol. Soc. Am. Bull.* **79**, 1151 (1968).
16. M. H. Carr, R. Greeley, *Volcanic Features of Hawaii: A Basis for Comparison with Mars* (U.S. Government Printing Office, Washington, DC, 1980).
17. M. T. Mellon, *J. Geophys. Res.* **102** (E11), 25617 (1997).
18. P. H. Smith *et al.*, *Science* **325**, 58 (2009).
19. J. S. Levy, D. R. Marchant, J. W. Head, *Icarus* **206**, 229 (2010).
20. W. V. Boynton *et al.*, *Science* **297**, 81 (2002).
21. T. R. Watters *et al.*, *Science* **318**, 1125 (2007).
22. J. Zimbelman, W. Garry, J. E. Bleacher, L. S. Crumpler, *Lunar Planet. Sci. Conf.* **42**, 2443 (2011).
23. G. P. Walker, *Bull. Volcanol.* **53**, 546 (1991).
24. K. Hon, J. Kauahikaua, R. Denlinger, K. Mackay, *Geol. Soc. Am. Bull.* **106**, 351 (1994).
25. D. L. Peck, *U.S. Geol. Surv. Prof. Pap.* **550B**, 148 (1966).
26. J. P. Lockwood *et al.*, *U.S. Geol. Surv. Prof. Pap.* **1613**, 1 (2000).
27. S. Thorpe, *J. Fluid Mech.* **46**, 299 (1971).
28. L. Keszthelyi *et al.*, *Geochem. Geophys. Geosyst.* **5**, Q11014 (2004).
29. R. F. Katz, R. Ragnarsson, E. Bodenschatz, *N. J. Phys.* **7**, 37 (2005).
30. Video of spiraling microplate formation in wax spreading center model by (*29*) may be viewed here: http://opscience.iop.org/1367-2630/7/1/037/media/movie.mpg.

Acknowledgments: We thank A. C. Enns, K. X. Whipple, and A. B. Clarke for insightful conversation during the preparation of this manuscript and R. Greeley, whose guidance prompted this work. All original data reported in this paper are archived by NASA's Planetary Data System.

20 January 2012; accepted 27 March 2012
10.1126/science.1219437

Organic Synthesis via Irradiation and Warming of Ice Grains in the Solar Nebula

Fred J. Ciesla[1]* and Scott A. Sandford[2]

Complex organic compounds, including many important to life on Earth, are commonly found in meteoritic and cometary samples, though their origins remain a mystery. We examined whether such molecules could be produced within the solar nebula by tracking the dynamical evolution of ice grains in the nebula and recording the environments to which they were exposed. We found that icy grains originating in the outer disk, where temperatures were less than 30 kelvin, experienced ultraviolet irradiation exposures and thermal warming similar to that which has been shown to produce complex organics in laboratory experiments. These results imply that organic compounds are natural by-products of protoplanetary disk evolution and should be important ingredients in the formation of all planetary systems, including our own.

Complex organic compounds have been found in meteorites and interplanetary dust particles, leading many to suggest that Earth's prebiotic material was delivered by comets and chondritic planetesimals. The origin of these organic compounds, however, is unknown. Whereas organic molecules can be produced during aqueous alteration of a parent body (*1*) or through Fischer-Tropsch reactions in protoplanetary disks (*2*), the high D/H ratios found in meteoritic organics point to a low-temperature origin (*3*). Irradiation of astrophysical ice analogs (containing simple molecules like H_2O, CO, CO_2, NH_3, and CH_3OH) by ultraviolet (UV) photons in the laboratory has produced of a suite of organic molecules similar to those found in primitive bodies in our solar system, including amino acids, amphiphiles, quinones, and nucleobases (*4*–*10*). These experiments simulated conditions (temperatures, pressures, radiation fluxes) similar to those found in dark molecular clouds—the collection of gas and dust that collapses to form stars and planets. Within these clouds, ice-mantled grains are exposed to relatively low fluxes of UV from the ambient interstellar radiation field, allowing organics to be produced. It remains unclear, however, if the full suite of complex organics found in primitive bodies could be produced within a molecular cloud and to what extent the compounds were preserved during the formation of the solar system.

These experimental conditions are also relevant to the outer solar nebula, where temperatures were low enough for C-, H-, O-, and N-bearing ices to form (*11*). If ices in this region were irradiated to substantial levels, organics would have been produced, increasing the inventory of such compounds beyond what may have been inherited from the molecular cloud. Indeed, observations of molecular emission features suggest that protoplanetary disks support active organic chemistry, processing the raw materials from the molecular cloud to yield higher abundances of organic species, though the pathways for production are unclear (*12*).

To investigate the production of organics after molecular-cloud collapse, we modeled the paths of ice-mantled grains through the solar nebula (Fig. 1) (*13*–*16*). Particles migrated around the nebula due to disk evolution, gas drag, gravitational settling, and both radial and vertical turbulent diffusion. We assumed that the level of turbulence in the disk is characterized by the turbulence parameter, α, which describes both the viscosity in the disk, $\nu = \alpha c_s H$ where c_s is the local speed of sound in the disk and H is the local gas scale height, and the diffusivity of trace materials, D (~ν) (*16*, *17*). We set $\alpha = 0.001$ everywhere, as the magnetorotational instability is expected to have operated in the outer disk (*18*).

The disk was assumed to be in a steady state and had a surface density distribution $\Sigma(r) = 2000\left(\frac{r}{1\ \mathrm{AU}}\right)^{-1}$ g/cm^2 [amounting to $^1/_{10}$ of the solar mass out to 70 astronomical units (AU)] and a thermal structure $T(r) = 200\left(\frac{r}{1\ \mathrm{AU}}\right)^{-\frac{1}{2}}$ K (where r is the distance from the Sun), appropriate for flared disks around young T Tauri stars (*11*, *19*). We tracked the dynamics of 5000 ice-mantled grains with radius a = 1 μm and unit density. Although particles of a broad range of sizes would have been present, we chose to follow 1-μm particles as individual organic hot spots, and globules in meteorites and comets are often found to be of this spatial scale (*20*, *21*). Particles began at the midplane of the disk (with the height above the disk midplane given by z, and the midplane defined as $z = 0$ AU) where $T = 30$ K ($r = 49$ AU). At this temperature, C- and N-bearing ices of the type needed to form organics condensed (*22*), and D/H ratios in water are elevated due to ion-molecule reactions (*23*).

[1]Department of the Geophysical Sciences, University of Chicago, 5734 South Ellis Avenue, Chicago, IL 60430, USA. [2]NASA Ames Research Center, MS 245-6, Moffett Field, CA 94035, USA.

*To whom correspondence should be addressed. E-mail: fciesla@uchicago.edu

whereas counterclockwise-in coils record left-lateral shear (*25*, *26*).

Both types of subaerial lava coils are present in HiRISE image PSP_007250_1840. They are concentrated near the centers of ~50- to 800-m-wide troughs. Chains of small, like-oriented coils (~4 m wide) with raised centers appear to be present along linear shear zones (Fig. 2B). Such coils may be voluted strips of plastic crust, as described above. Within the smaller northwest-southeast trending trough, coil chains are counterclockwise-oriented (e.g., Figure 2B), indicative of a left-lateral shearing pattern. The larger (>10 m wide), coplanar lava coils are more likely formed by means of the latter mechanism discussed above. These coils are abundant within the wide, southwest-northeast trending trough. Here, the orientations are mixed but predominantly clockwise, indicative of more complex flow patterns with a less substantial overall right-lateral shear.

The troughs themselves appear to have fractured into "secondary plates" that drifted apart in several locations (Fig. 4). As with the primary plates, the direction of secondary-plate movement may be inferred from the plate geometry. When the pieces of the puzzle are reassembled, it is also apparent that the polygons and coils on these plates are continuous across the fracture zones and that these surface features must have been present before this secondary-plate drift occurred. The overall patterns of the primary and secondary plates' motion are consistent with directions of shear inferred from spiral orientation.

All of the aforementioned features and inferred processes are best explained by volcanic, rather than ice, processes. The primary plates likely formed as an early solidification crust atop a lava flow. As this crust fractured and drifted apart, underlying molten lava was exposed. Lava coils formed on the cooling surface in the shear zones between the primary plates. Some coils were eventually preserved in the flow crust as it fully solidified and fractured into the network of polygons that we observe in the troughs today. In several locations, these secondary, patterned plates then fractured into smaller plates, thus exposing more molten lava and allowing the process of lava coil and crust formation to repeat.

Ice-related processes fail to account for our observations. There are no known mechanisms to naturally produce spiral patterns in ice-rich environments on the scale and frequency observed in our study area. If the primary plates were ice rafts, then the water extruded during rafting would not have the correct viscosity to form and preserve the coils. We have also shown that the polygons formed after the fracture and drift of the secondary plates on which they are present. This precludes the notion that the polygons formed over decades or even centuries in an ice-rich regolith, because it seems unlikely that frozen soil could somehow fracture and drift.

The patterns of the primary and secondary plates' movement are morphologically similar to historical platy-ridged Icelandic lava flows (*28*). The troughs also contain other features that are indicative of volcanism, such as sinuous pressure ridges (Fig. 2C). In several locations, the secondary plates have been pushed up from below, sometimes causing them to crack (Fig. 5). We suggest that these are tumuli or evidence of flow deflation and draping of the plates on underlying topographic highs (*23*). A large fracture on one such feature exposes the edge of a secondary plate that is ~2.5 m thick (Fig. 5B).

The secondary plates contain many linear to meandering depressions up to 10 m wide (Fig. 2B). One depression runs across the entire observable length (~2 km) of the narrow trough in Fig. 2A and is interpreted to be an incipient rift in a secondary plate. The chain of coils in Fig. 2C are connected by curvilinear depression in an arrangement similar to wax models of rotating microplate formation in sea-floor spreading centers (*29*, *30*). This spreading-center style of plate formation, on a smaller scale, may have led to coil and secondary-plate formation in areas like Figs. 2C and 4, where minor lateral translation influenced coil orientation.

We conclude that the lava coils, polygons, and primary/secondary plates in Cerberus Palus are primary volcanic structures. It is likely that lava coils and evidence of secondary-plate motion are fairly common in Cerberus Palus. Despite differences in aeolian cover, the primary and secondary plates are presumed to have developed within contemporaneous flow events. However, it is unclear whether the multiple generations of

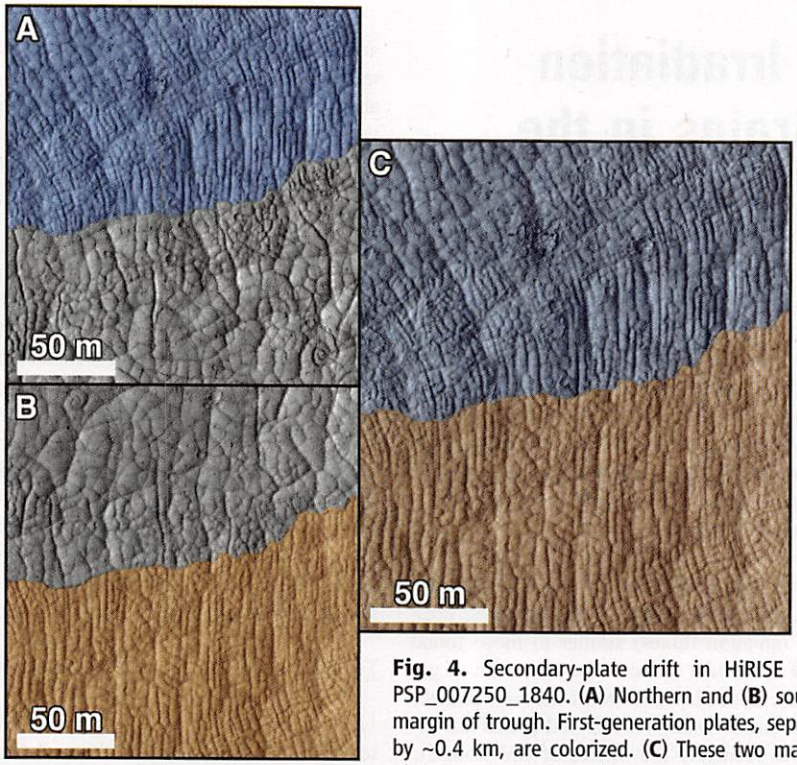

Fig. 4. Secondary-plate drift in HiRISE image PSP_007250_1840. (**A**) Northern and (**B**) southern margin of trough. First-generation plates, separated by ~0.4 km, are colorized. (**C**) These two marginal plates are continuous when sutured together.

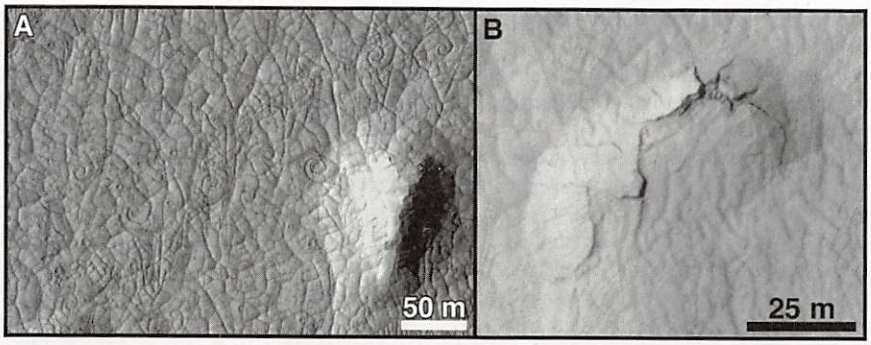

Fig. 5. HiRISE image PSP_007250_1840. (**A**) Raised crust next to complex chain of clockwise and counterclockwise coils. (**B**) Edge of uplifted crust is fully exposed.

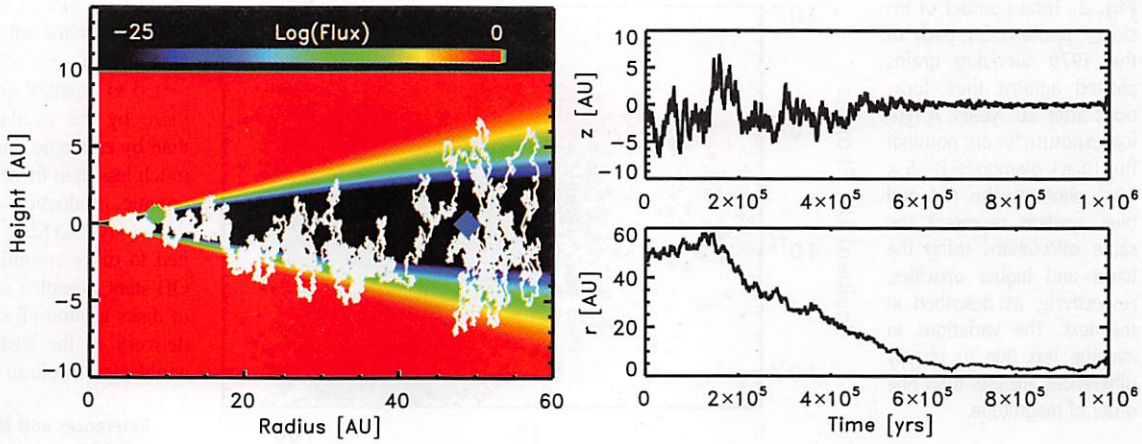

Fig. 1. (**Left**) Trajectory of one of the surviving particles (which are defined as those that did not migrate inside of 0.1 AU of the young Sun) through the solar nebula superimposed on a map of the UV radiation flux in the disk. The flux is normalized to its value at $z = \pm\infty$ and assumed to propagate normal to the disk midplane. The blue and green symbols denote the starting and final locations, respectively. (**Right**) The r and z coordinates of the particle through time.

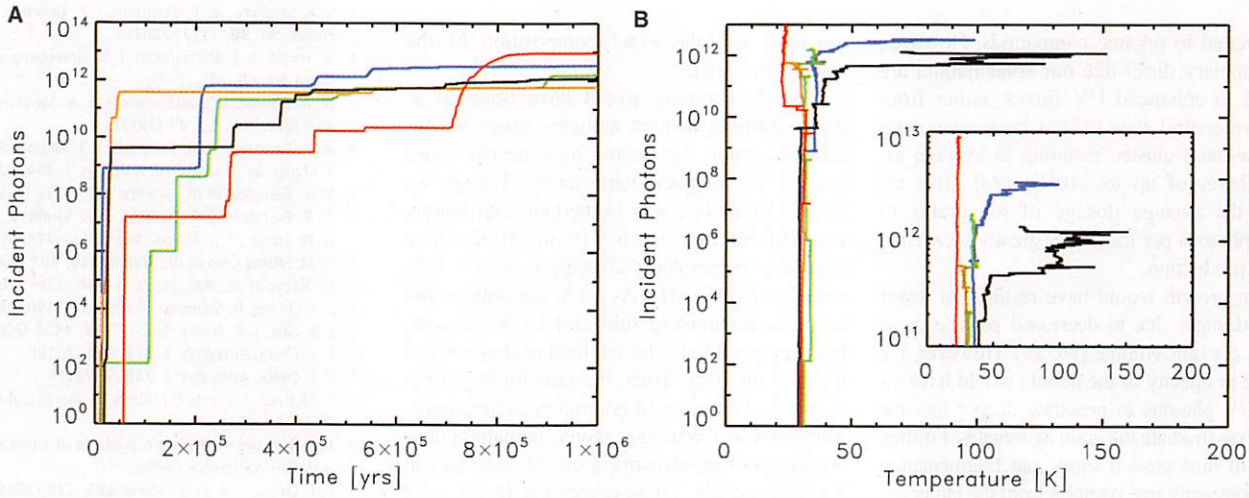

Fig. 2. (**A**) Cumulative number of photons incident on five grains throughout the 10^6-year lifetime in the disk, assuming an incident flux of $1G_0$. The black curve corresponds to the grain whose trajectory is shown in Fig. 1; the other curves represent other random particles from the simulation. (**B**) Total incident photons seen by the same particles plotted against their temperatures. The inset shows a zoomed-in view.

As a particle moved through the disk, we calculated the number of UV photons incident on its surface. The radiation was assumed to be incident on the disk with a flux, F_0, directed normal to the disk midplane. The flux was attenuated with depth as photons were absorbed by solid particles. Thus, the flux everywhere was $F(r,z) = F_0 e^{-\tau(r,z)}$, where τ is the optical depth of material suspended in the disk above the point of interest [$\tau(r,z) = \int_{|z|}^{\infty} \rho_g(r,z)\kappa dz$, where $\rho_g(r,z)$ is the density of material in the disk and κ is the average opacity of the suspension]. We assume an opacity of $\kappa = 7.5$ cm^2/g, a conservative value that is on the high end of the range expected in the cool outer regions of a protoplanetary disk (*24*). Lower opacities would increase the number of photons seen by each particle. We take as a baseline an incident flux equivalent to the current interstellar UV flux of 10^8 photons cm^{-2} s^{-1} ($1G_0$) (*25*), but higher fluxes can be considered by multiplying by the desired enhancement factor.

The starting location of the particles was shielded such that the flux was attenuated by more than 25 orders of magnitude. As most of the mass of the nebula was located around the midplane, these conditions are often used in calculating the chemical evolution of primitive materials. At this location, an ice grain would have seen $<10^{-25} F_0 \pi a^2 \Delta t \sim 10^{-11}$ photons if it remained at its starting location throughout the simulation, a period of $\Delta t = 10^6$ years. However, in the presence of vertical diffusion, small particles spend ~68% of their time within $1H$ of the midplane but 32% of their lifetimes at higher altitudes, with ~5% being spent above $2H$ (*14*). Because the UV flux was a strong function of height, it was the infrequent but non-negligible excursions to high altitudes that were primarily responsible for small grains seeing large numbers of photons. Irradiation exposures also increased as grains diffused outward in the disk, where the lower surface densities of gas and dust allowed the UV to penetrate closer to the disk midplane. Thus, the radial and vertical motions of the grains controlled their UV exposures.

Figure 2 shows that the cumulative number of UV photons grains encountered did not climb uniformly. Rather, the increases in incident photons were episodic and occurred when a grain was lofted to high altitudes or far out in the disk. Plotting the irradiation histories against the temperatures seen by the particles, where we took the particle temperature as being equal to the gas temperature everywhere, demonstrates how the UV exposure generally rose early while the grains were cold and when all key ices remained on the grain. Less than 0.5% of photons would desorb these molecules (*26*), which would then recondense on the same or another grain. Thus, loss of mass in this manner would be minimal.

Figure 3 shows that a typical dosage for the particles was ~5×10^{12} photons in our nominal case. Assuming a pure H_2O grain, this corresponds to ~50 UV photons per molecule. Experimental results suggest an efficiency of production of approximately one organic molecule produced per 400 incident photons (*6*, *16*). Thus >12% of the mass of ices in the outer solar nebula would

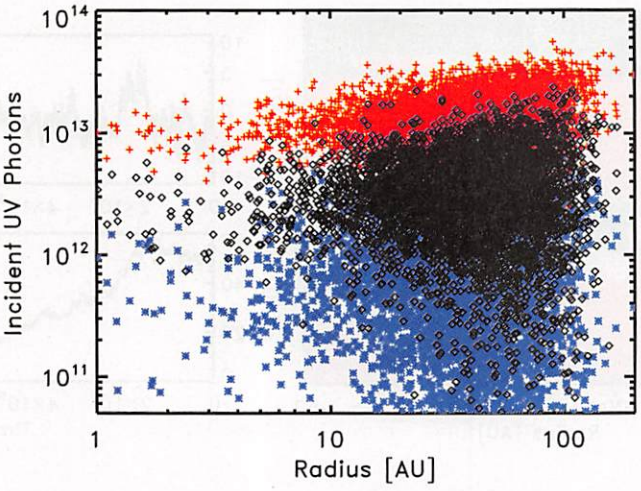

Fig. 3. Total number of incident photons for each of the 4979 surviving grains plotted against their locations after 10^6 years. A typical exposure for our nominal flux (black diamonds) is ~5 × 10^{12} photons. The red and blue symbols represent the same calculations using the lower and higher opacities, respectively, as described in the text. The variations in average flux due to opacity differences are less than one order of magnitude.

be converted to organic compounds. However, protoplanetary disks like our solar nebula are exposed to enhanced UV fluxes, either from their own central stars (*27*) or from other stars in a low-mass cluster, resulting in average incident fluxes of up to ~$10^3 G_0$ (*28*). This increases the average dosage of ice grains to 50,000 photons per molecule, greatly increasing organic production.

Grain growth would have resulted in lower photon dosages due to decreased particle cross sections per unit volume (*16*, *29*). However, the decrease in opacity of the nebula would have allowed UV photons to penetrate deeper into the disk (*29*) to irradiate the grain aggregates. Further, models of dust growth show that fragmentation would constantly free particles from the larger aggregates through energetic collisions (*30*). Thus, even if icy grains remain as 1-μm entities for just a part of the 10^6 years modeled here, they can receive substantial UV dosages (Fig. 2).

By itself, irradiation does not produce the organic compounds. When UV photons are incident on astrophysical ices in the laboratory, they break molecular bonds in the ices, producing reactive ions and radicals. If these reactive photoproducts are adjacent to each other, they may react to form new compounds, even at very low temperatures. When the irradiated ice is warmed, the photoproducts become mobile and react more readily. Such reactions occur during warm-ups through any temperature range but are particularly enhanced during the amorphous-amorphous transition near 80 K, the amorphous-to-cubic transformation around 135 K, and the sublimation of the H_2O in the ice at $T > 135$ K (*4*–*10*, *16*). Thus, warming of irradiated ices yields a burst of organic synthesis, even if the ice is not currently being irradiated. Reactions brought on by warming are still largely constrained by proximity rather than considerations of normal chemical equilibrium. However, these experimental results are robust in that the amounts and types of molecules produced are largely insensitive to the temperature of the ices during irradiation and the exact composition of the starting ices (*16*).

Particle warming would have occurred as grains diffused to high altitudes where the increased photon flux would have heated grains beyond the midplane temperature. Though we assumed our disk was isothermal with height, temperatures may reach ~10 to 50 K above midplane temperatures at heights of $|z| > 0.2r$ outside ~10 AU (*31*). As such, not only would particles accumulate substantial UV dosages, but they would also be warmed as they moved through the disk. Thus, the conditions shown to produce organics in laboratory experiments, irradiation and warming, would be natural consequences of the dynamical evolution of ices in the solar nebula. Photo-processing in the solar nebula thus represents an ideal environment for this form of organic synthesis.

The grains in our study are irradiated during their large-scale movement in the disk, which suggests that similar products would be made available to meteoritic and cometary bodies, consistent with observations (*20*, *21*). Further, organics on particles brought to the innermost regions of a protoplanetary disk would vaporize, allowing the products of this organic chemistry to be observed in the gas phase, offering an explanation for the emission features observed by the Spitzer Space Telescope (*12*). As we predict that complex species such as amino acids will be formed, identification of more complex organic species in other disks may serve to test this method of production. Because the total UV fluences received by ices in the solar nebula are considerably greater than those experienced by typical ices in dense molecular clouds, disk processing would yield greater overall conversions of ices into organics and would produce organics of greater complexity. The exact mass of organic production remains uncertain, as it will depend on the incident UV flux and the mass of ice contained in the outer disk. Our results, however, demonstrate that cold, icy 1-μm grains would see UV dosages of ~10^{12} to 10^{15} photons for modest incident fluxes of 1 to $10^2 G_0$. This allows for substantial organic production, with at least ~5% of the mass of ices being converted to organics and production being limited more by the availability of starting materials than by energetic photons (*16*). These fluxes are much less than those thought to be necessary for organic production to occur in protoplanetary disks (~$10^6 G_0$) (*29*). Thus, rather than being limited to disks around stars located near massive OB stars, complex organics should be produced in disks around all stars and made available for delivery to the surface of planets where they could play a role in the origin of life.

References and Notes

1. E. T. Peltzer, J. L. Bada, G. Schlesinger, S. L. Miller, *Adv. Space Res.* **4**, 69 (1984).
2. J. A. Nuth III, N. M. Johnson, S. Manning, *Astrophys. J.* **673**, L225 (2008).
3. S. A. Sandford, M. P. Bernstein, J. P. Dworkin, *Meteorit. Planet. Sci.* **36**, 1117 (2001).
4. W. Hagen, L. J. Allamandola, J. M. Greenberg, *Astrophys. Space Sci.* **65**, 215 (1979).
5. W. A. Schutte, L. J. Allamandola, S. A. Sandford, *Adv. Space Res.* **12**, 47 (1992).
6. M. P. Bernstein, S. A. Sandford, L. J. Allamandola, S. Chang, M. A. Scharberg, *Astrophys. J.* **454**, 327 (1995).
7. M. P. Bernstein *et al.*, *Science* **283**, 1135 (1999).
8. M. P. Bernstein, J. P. Dworkin, S. A. Sandford, G. W. Cooper, L. J. Allamandola, *Nature* **416**, 401 (2002).
9. G. M. Muñoz Caro *et al.*, *Nature* **416**, 403 (2002).
10. M. Nuevo *et al.*, *Adv. Space Res.* **48**, 1126 (2011).
11. E. I. Chiang, P. Goldreich, *Astrophys. J.* **490**, 368 (1997).
12. J. S. Carr, J. R. Najita, *Science* **319**, 1504 (2008).
13. F. J. Ciesla, *Astrophys. J.* **723**, 514 (2010).
14. F. J. Ciesla, *Astrophys. J.* **740**, 9 (2011).
15. S. Charnoz, L. Fouchet, J. Aleon, M. Moreira, *Astrophys. J.* **737**, 33 (2011).
16. Materials and methods are available as supplementary materials on *Science* Online.
17. F. J. Ciesla, J. N. Cuzzi, *Icarus* **181**, 178 (2006).
18. T. Sano, S. M. Miyama, T. Umebayashi, T. Nakano, *Astrophys. J.* **543**, 486 (2000).
19. L. Hartmann, N. Calvet, E. Gullbring, P. D'Alessio, *Astrophys. J.* **495**, 385 (1998).
20. S. A. Sandford *et al.*, *Science* **314**, 1720 (2006).
21. K. Nakamura-Messenger, S. Messenger, L. P. Keller, S. J. Clemett, M. E. Zolensky, *Science* **314**, 1439 (2006).
22. K. Lodders, *Astrophys. J.* **591**, 1220 (2003).
23. K. Willacy, *Astrophys. J.* **660**, 441 (2007).
24. Z. Zhu, L. Hartmann, C. Gammie, *Astrophys. J.* **694**, 1045 (2009).
25. H. J. Habing, *Bull. Astron. Inst. Neth.* **19**, 421 (1968).
26. K. Öberg, H. Linnartz, R. Visser, E. F. van Dishoeck, *Astrophys. J.* **693**, 1209 (2009).
27. T. J. Bethell, E. A. Bergin, *Astrophys. J.* **739**, 78 (2011).
28. F. C. Adams, E. M. Proszkow, M. Fatuzzo, P. C. Myers, *Astrophys. J.* **641**, 504 (2006).
29. H. B. Throop, *Icarus* **212**, 885 (2011).
30. S. J. Weidenschilling, *Icarus* **60**, 553 (1984).
31. P. Woitke, I. Kamp, W.-F. Thi, *Astron. Astrophys.* **501**, 383 (2009).

Acknowledgments: F.J.C. and S.A.S. acknowledge funding from NASA's Origins of Solar Systems program. S.A.S. also thanks the Astrobiology Institute for funds.

Supplementary Materials

www.sciencemag.org/cgi/content/full/science.1217291/DC1
Supplementary Text
Figs. S1 to S11
References (*32*–*47*)

30 November 2011; accepted 13 March 2012
Published online 29 March 2012;
10.1126/science.1217291